Construction and Testing of GFRP Steel Hybrid-Reinforced Concrete Bridge-Deck Slabs of Sainte-Catherine Overpass Bridges

Ehab A. Ahmed, M.ASCE[1]; François Settecasi[2]; and Brahim Benmokrane[3]

Abstract: Hybrid reinforcement for concrete bridge-deck slabs is being investigated through a collaboration project between the Ministry of Transportation of Quebec (MTQ) and the University of Sherbrooke. This paper presents design concepts, construction details, and results of live-load field tests of the twin hybrid-reinforced bridges (P-15502N and P-15502S) on Sainte Catherine Road in Sherbrooke, Quebec (Canada). These hybrid-reinforced slab-on-girder bridges are simply supported over a single span of 43,415 mm. Their 200-mm-thick concrete deck slabs are continuous over four spans of 2,650 mm each, with an average overhang of about 1,000 mm on both sides (measured perpendicular to the girder axis). The deck slabs were reinforced with glass fiber–reinforced polymer (GFRP) reinforcing bars in the top mat and with galvanized steel bars in the bottom mat. One of the two bridges (P-15502S) was instrumented with fiber-optic sensors (FOSs) in the bridge-deck slab (over and between the girders). The instrumented bridge was tested for service performance with three calibrated truck loads prior to placement of the asphalt layer to check for flexural cracks. The construction details and the results of the live-load field tests are presented. The field tests yielded very small strains in the GFRP reinforcing bars, which clarified the arch-action effect in the restrained hybrid-RC bridge decks. **DOI:** 10.1061/(ASCE)BE.1943-5592.0000581. © *2014 American Society of Civil Engineers.*

Author keywords: Bridges; Concrete; Bridge decks; Highway; Fiber-reinforced polymer (FRP); Glass fibers; Reinforcement; Field tests; Strain; Deflection; Arch action; Monitoring.

Introduction

Most RC bridges in Canada are of slab-on-girder type. The deck slabs of these bridges are reinforced with two mats (top and bottom) and connected to the supporting girders with shear connectors (studs). Because of the harsh environmental conditions and the excessive use of deicing salts in the winter, the steel-reinforced concrete bridge-deck slabs exhibit steel corrosion and consequent deterioration. The costs of the repairs and related problems, such as delaying and detouring traffic, have provided an impetus to use noncorrosive fiber-reinforced-polymer (FRP) bars as an alternative reinforcement.

Since 1992, significant efforts have been made in Canada to significantly change the design and construction of bridge structures by developing innovative structures incorporating FRPs, fiber-optic sensors (FOSs), and structural health monitoring (SHM) (Mufti and Neale 2007). The Structures Division of the Ministry of Transportation of Quebec (MTQ), since the late 1990s, has been interested in building bridges with an extended service life of 75–150 years. These durable bridges can be built by employing noncorroding FRP reinforcing bars as the main reinforcement for the concrete bridge decks. Based on this technique, the MTQ has carried out, in collaboration with the University of Sherbrooke (Sherbrooke, Quebec), several research projects using FRP reinforcement in concrete bridge-deck slabs under static and fatigue loadings (El-Gamal et al. 2005, 2007; El-Ragaby et al. 2007a, b) and bridge barriers under static and impact loadings (El-Salakawy et al. 2003a, 2004; Ahmed and Benmokrane 2011; Ahmed et al. 2013). Moreover, several demonstration field applications have been carried out in Quebec, such as the Joffre Bridge in Sherbrooke, the Wotton Bridge in Wotton, the Magog Bridge on Highway 55 North, the Cookshire-Eaton Bridge on Route 108, and the Val-Alain Bridge on Highway 20 East (El-Salakawy and Benmokrane 2003; El-Salakawy et al. 2003b, 2005; Benmokrane et al. 2004, 2007), and in the United States, such as Morristown Bridge in Vermont (Benmokrane et al. 2006) and the bridges located at Pierce Street in Lima (Ohio 1999), Salem Avenue in Dayton (Ohio 1999), Rollins Road in Rollinsford (New Hampshire 2000), Sierrita de la Cruz Creek in Potter County (Texas 2000); 53rd Avenue in Bettendorf (Iowa 2001), Bridge Street in Southfield (Michigan 2001), Highway 151 in Waupun (Wisconsin 2005), and Route Y in Boone County (Missouri 2007) (Eamon et al. 2012). Most of these projects focused on the use of the glass-FRP (GFRP) bars because of their relatively lower cost compared with that of other FRPs (carbon and aramid). Some of these bridges have been in service for more than 10 years without any signs of deterioration or unexpected problems. Furthermore, the durability of GFRP reinforcement in real RC bridges exposed to different environments for 10–13 years has been investigated (Mufti et al. 2005, 2007, 2011). The investigations (Mufti et al. 2005, 2007, 2011) showed that the structure of the polymer matrix of GFRP reinforcement was not significantly disrupted by exposure to the environment. Neither hydrolysis nor significant changes in the glass

[1]Postdoctoral Fellow, Dept. of Civil Engineering, Univ. of Sherbrooke, Sherbrooke, QC, Canada J1K 2R1. E-mail: ehab.ahmed@usherbrooke.ca

[2]Master's Student, Dept. of Civil Engineering, Univ. of Sherbrooke, Sherbrooke, QC, Canada J1K 2R1. E-mail: francois.settecasi@usherbrooke.ca

[3]Natural Sciences and Engineering Research Council (NSERC) and Tier-1 Canada Research Chair Professor in Advanced Fiber-Reinforced Polymer Composite Materials for Civil Structures, Dept. of Civil Engineering, Univ. of Sherbrooke, Sherbrooke, QC, Canada J1K 2R1 (corresponding author). E-mail: brahim.benmokrane@usherbrooke.ca

Note. This manuscript was submitted on May 13, 2013; approved on November 7, 2013; published online on January 10, 2014. Discussion period open until June 10, 2014; separate discussions must be submitted for individual papers. This paper is part of the ***Journal of Bridge Engineering***, © ASCE, ISSN 1084-0702/04014011(11)/$25.00.

transition temperature of the matrix took place after exposure to the combined effects of the concrete alkaline environment and the external natural environmental exposure for 10–13 years. These compelling pieces of evidence presented on the durability of GFRP reinforcement encourage wider acceptance of this technology in new applications with extended service life.

In a typical slab-on-girder concrete bridge deck, the top reinforcing mat is closer to the concrete surface and, consequently, is susceptible to chloride and chemical exposure, which may accelerate the corrosion of the steel bars. The bottom reinforcement mat, however, is not susceptible to such exposure. In addition, the design of these bridge decks controls crack width, which limits chloride migration from the top surface to the bottom reinforcement layer. Thus, design engineers and municipalities proposed to use noncorrosive GFRP bars in the top reinforcement mat and maintain steel bars in the bottom reinforcement mat (hybrid-reinforced-concrete bridge-deck slabs). This technique is expected to yield durable concrete bridge decks with cost-effective designs, because only the top reinforcing mat is replaced with GFRP bars.

The Canadian Standards Association (CSA) (2006), which allows the use of GFRP bars as the main reinforcement in bridge-deck slabs, provides a step forward toward the transition from research to commercial projects based on cost-benefit considerations. Consequently, there is a remarkable increase in the use of FRPs in bridges such as Hawk Lake bridge (Ontario 2008), Bridgeport bridge and Dry Sadle bridge (Ontario 2009), Shadow River bridge (Ontario 2010), and 18th Street bridge (Manitoba 2010). The CSA (2006) provides two different design methods for the bridge-deck slabs, namely, the flexural design method and empirical method. These design methods are for bridge-deck slabs totally reinforced with steel or FRP bars. The code, however, makes no provisions for the hybrid reinforcement concept. Consequently, there is a need to understand how these hybrid-reinforced-concrete bridge-deck slabs perform and then to approve and integrate this concept into bridge design codes and guidelines.

To investigate the effectiveness and durability of GFRP bars as top reinforcement for concrete decks, the Virginia Department of Transportation (VDOT) and the Virginia Transportation Research Council (VTRC) with funding provided through the Federal Highway Administration's (FHWA) Innovative Bridge Research and Construction (IBRC) program worked with Virginia Tech to construct the Route 668 Bridge over Gills Creek in Franklin County, Virginia. The bridge was completed in July 2003. The deck of one span was reinforced with GFRP bars for the top mat and epoxy-coated steel bars for the bottom mat. The other two spans were reinforced with epoxy-coated steel bars for the top and bottom mats (Phillips et al. 2005). Live-load tests were performed in 2003 shortly after the completion of construction and again in 2004. In addition, tests were performed on the deck of the opposite end-span, which had all epoxy-coated steel reinforcement. The performances of the two end-spans were compared to determine if the GFRP reinforcement had any significant influence on the overall bridge behavior compared with the epoxy-coated steel bars. Phillips et al. (2005) reported that there were no significant differences in the behavior of the deck after 1 year of service, and there was no visible cracking. The behavior of the two end-spans was similar, and the measured girder distribution factors were less than the AASHTO design recommendations. Recently, the MTQ initiated an extensive research project in collaboration with the University of Sherbrooke aimed at investigating the structural performance of hybrid-reinforced-concrete bridge decks through some new concrete bridges that are being built along the extension of Highway 410 (Sherbrooke, Quebec). The first in this series was the 410 overpass on Boulevard de l'Université in Sherbrooke, which was built and tested in 2010 (Ahmed and Benmokrane 2012), followed by the Sainte Catherine twin overpasses (P-15502N and P-15502S; Sherbrooke, Quebec), which were constructed in 2012.

This paper presents the design criteria and investigates the service performance of the Sainte Catherine twin overpasses (P-15502N and P-15502S; Sherbrooke, Quebec) through a live-load field test of the P-15502S bridge, which was instrumented with FOSs. The results reported in this paper provide a step forward toward introducing the hybrid-reinforcement technique to the bridge design codes and guides.

Project Description and Construction

The Sainte Catherine twin overpass bridges (P-15502N and P-15502S) are located on Highway 410 in Sherbrooke, passing over Sainte Catherine Road in Quebec, Canada. The project comprises two identical bridges (Highway 410 East and Highway 410 West) with a typical slab-on-girder structural system. Each bridge has two traffic lanes (see layout in Fig. 1). Each bridge has five steel girders simply supported over a single span of 43,415 mm [Fig. 2(a)]. The concrete deck slab is 200 mm thick [Fig. 2(b)] and continuous over four 2,650-mm spans with an average overhang of about 10 mm on each side (measured perpendicular to the girder axis).

The main steel girders of the two bridges are composite with the concrete deck slab using 22-mm-diameter × 130-mm-long stud connectors. The steel girders have a constant depth of 1,700 mm over the span. The steel girders are supported laterally using six cross frames spaced at 5,873 mm. The top mat of the concrete deck slab was reinforced with sand-coated GFRP reinforcing bars manufactured by Pultrall (Thetford Mines, Quebec, Canada). The bottom reinforcing mat was made of galvanized steel bars. The side barriers of the two bridges were of MTQ 210 type (steel post and beam over a concrete curb) and were reinforced with galvanized steel bars.

The construction of the slabs of the twin overpass bridges (P-15502N and P-15502S) started on April 2012 with the setting up of the formwork for the deck slabs for the two bridges. Fig. 3 shows the different stages of construction. Because of the light weight of the GFRP bars, more bars were handled in less time. Plastic support arrays spaced at 0.75 m were used to maintain bottom and top concrete clear covers of 38 and 50 mm, respectively. Neither the GFRP bars nor the steel bars were spliced in the transverse direction. On the other hand, there were three splices with a splice length of 600 mm ($\approx 30d_b$, where d_b is the reinforcing bar diameter) in the longitudinal steel bars in the bottom mat and three splices with a splice length of 960 mm ($\approx 50d_b$) in the longitudinal GFRP bars in the top mat. The additional GFRP bars at the overhang were placed between the continuous transverse top reinforcement elements and were extended 1.4 m into the adjacent span to ensure adequate development length and moment resistance. The placement of the bottom steel reinforcement mat was completed on May 18, 2012, and the top GFRP reinforcement mat was completed on May 22, 2012. The two bridge-deck slabs were cast on May 31, 2012, starting with the P-15502N bridge and ending with the P-15502S bridge (instrumented), which is the one being reported in this paper. Because one of the project's main objectives was to verify flexural cracking that might occur during field testing, the P-15502S bridge was tested before being paved. The live-load field test was conducted on October 30, 2012.

Design of the Bridge's Concrete Deck Slab

The bridge-deck slabs of the two bridges were designed according to the flexural design method in CSA (2006). The applicability of the

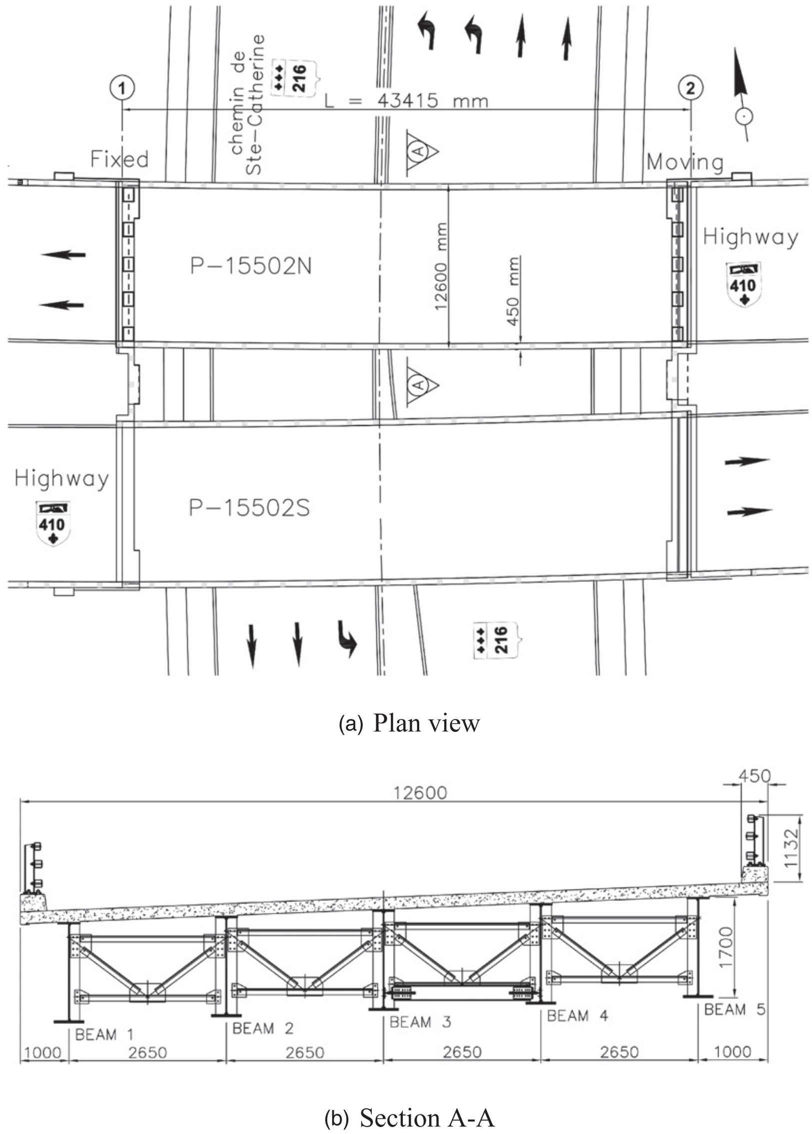

Fig. 1. Layout of the twin bridges: (a) plan view; (b) section A-A

empirical design method, however, was verified, and the bridge-deck slabs were designed accordingly to compare the reinforcement amounts resulting from both design methods.

Material Properties

Normal-strength concrete (Type V MTQ) with a 28-day concrete compressive strength of 35 MPa was used for the bridge-deck slab. Sand-coated GFRP bars were used for the top mat of the bridge-deck slab (No. 20, 19.1-mm diameter), whereas 15M and 20M galvanized steel bars were used for the bottom mat. The GFRP bars were manufactured by combining the pultrusion process and an in-line coating process for the outside surface. These bars were made of high-strength E-glass fibers with a fiber content of 85.5% (by weight) in a vinyl ester resin. The average ultimate tensile strength (f_{FRPu}) and the tensile modulus of elasticity (E_f) of the GFRP bars were 1,390 ± 8 MPa and 54.3 ± 0.8 GPa, respectively. Table 1 shows the properties of the GFRP and steel reinforcing bars.

Flexural Design Method

As mentioned earlier, the bridge's concrete deck slabs were designed according to the flexural design method in CSA (2006). The design bending moments were based on a maximum wheel load of 87.5 kN (CL-625 truck). The design service load for the deck slabs was taken as $1.4 \times 0.9 \times 87.5 = 110.25$ kN, where 1.4 is the impact coefficient and 0.9 is the live-load combination factor, whereas the design factored load was taken as $1.4 \times 1.7 \times 87.5 = 208.25$ kN, where 1.7 is the live-load combination factor. The service and ultimate moments over the girders and between the girders were 29.29 and 53.73 kN·m, respectively.

The deck slabs were designed considering serviceability and ultimate limit states. The crack width of the concrete slab and allowable stress limits were the controlling design factors. The maximum allowable crack width was 0.5 mm, and the stress in the GFRP bars was 25% of the ultimate strength of the GFRP bars (f_{FRPu}) under service loads (CSA 2006). The sections located over the girders (negative moment sections reinforced with GFRP No. 20 at 140 mm) were designed as overreinforced sections, and the resisting moment

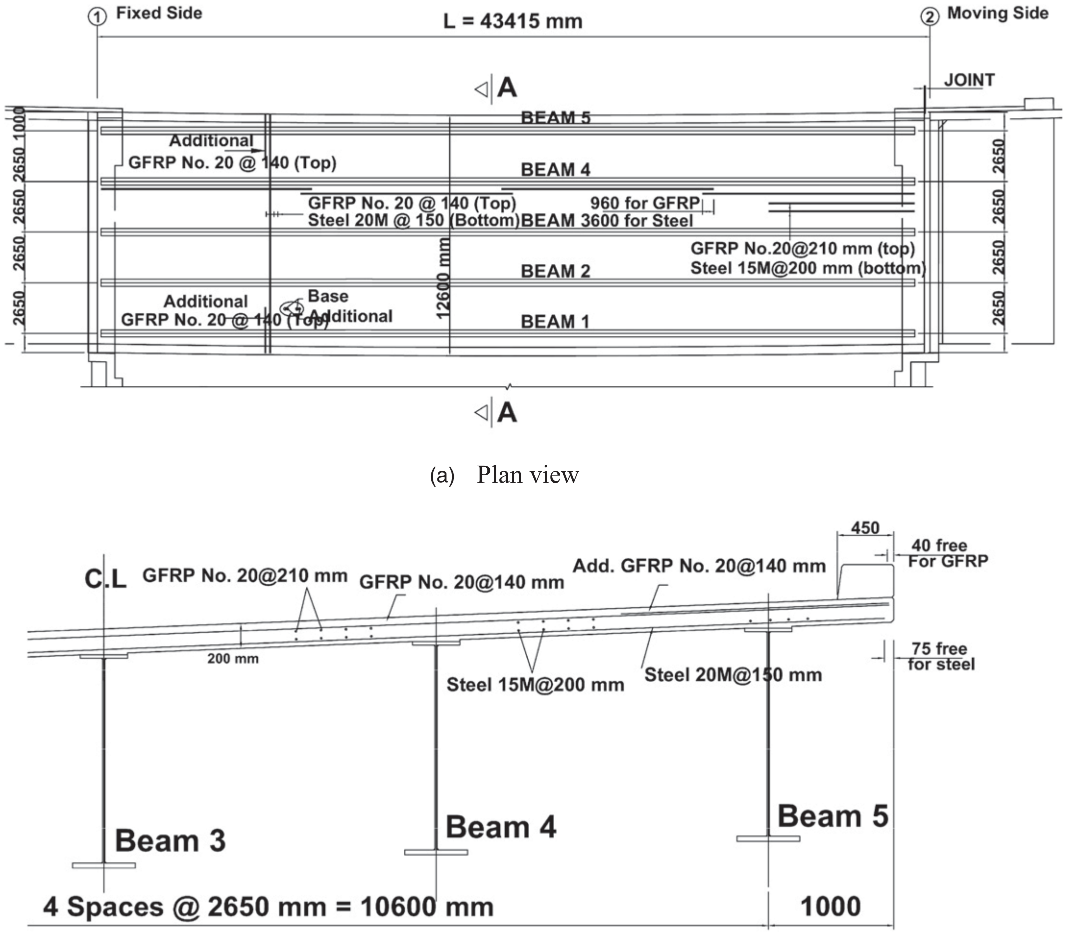

(a) Plan view

(b) Section A-A

Fig. 2. Geometry and reinforcement details: (a) plan view; (b) section A-A

(M_r) was 75.87 kN·m. At service load, the strain in the GFRP bars was 2,071 microstrains with a corresponding stress of 112.46 MPa, which is less than $0.25f_{\mathrm{FRPu}}$. The maximum crack width at service load was 0.47 mm, which is less than 0.5 mm.

Based on this design approach, the concrete bridge-deck slabs were entirely reinforced with two reinforcement mats comprised of No. 20 GFRP bars and 20M and 15M steel bars. For the bottom reinforcement mat, 20M steel bars were spaced at 150 mm in the transverse direction, and 15M steel bars were spaced at 200 mm in the longitudinal direction. For the top reinforcement mat, No. 20 GFRP bars spaced at 140 and 210 mm in the transverse and longitudinal directions, respectively, were used. Top and bottom clear concrete covers were 50 and 38 mm, respectively. Additional No. 20 GFRP bars spaced at 140 mm were placed in the top transverse layer at the two cantilevers [Fig. 2(b)] as well as in the top longitudinal layer at the ends of the deck slab.

Empirical Design Method

The bridges were also designed according to the empirical design method (CSA 2006) for comparison with the results of the flexural design method (CSA 2006). The bridge-deck slabs satisfied the requirements of the empirical method, which are as follows:

1. The bridge-deck slab was of uniform thickness and bounded by exterior supporting beams.
2. As shown in Fig. 1, the deck slab was composite with parallel supporting beams, and the lines of supports for the beams were also parallel to each other.
3. The ratio of the spacing of the supporting beams to the slab thickness was $(2.65/\cos\theta)/0.20 = 13.3 < 18.0$.
4. As shown in Fig. 1, the spacing of the supporting beams was <4.0 m, and the slab extended sufficiently beyond the external beams to provide a full development length for the bottom transverse reinforcement, because the cantilever length was more than $1/3$ of the adjacent span.
5. Longitudinal reinforcement in the deck slab in the negative-moment regions of the continuous composite beams was provided for in accordance with Clause 8.19.4 and Section 10, if applicable.

Thus, although these two bridge-deck slabs could have been designed using the empirical method, the MTQ has not used this bridge-design method to date. Considering the steel reinforcing bars, the area of steel reinforcing bars should be calculated according to CSA (2006, Clause 8.18.4.2), whereas the area of FRP reinforcing bars should be calculated according to CSA (2006, Clause 16.8.8.1).

Accordingly, the area of the bottom transverse reinforcing steel bars was equal to $\rho/\cos^2\theta \times d_s \times 1{,}000\ \mathrm{mm}^2/\mathrm{m}$, where ρ is the reinforcement ratio, which equals 0.003, θ is the skew angle, and d_s is the effective depth of the deck slab. This yields 15M steel bars at 300 mm as the bottom transverse reinforcement, which is the

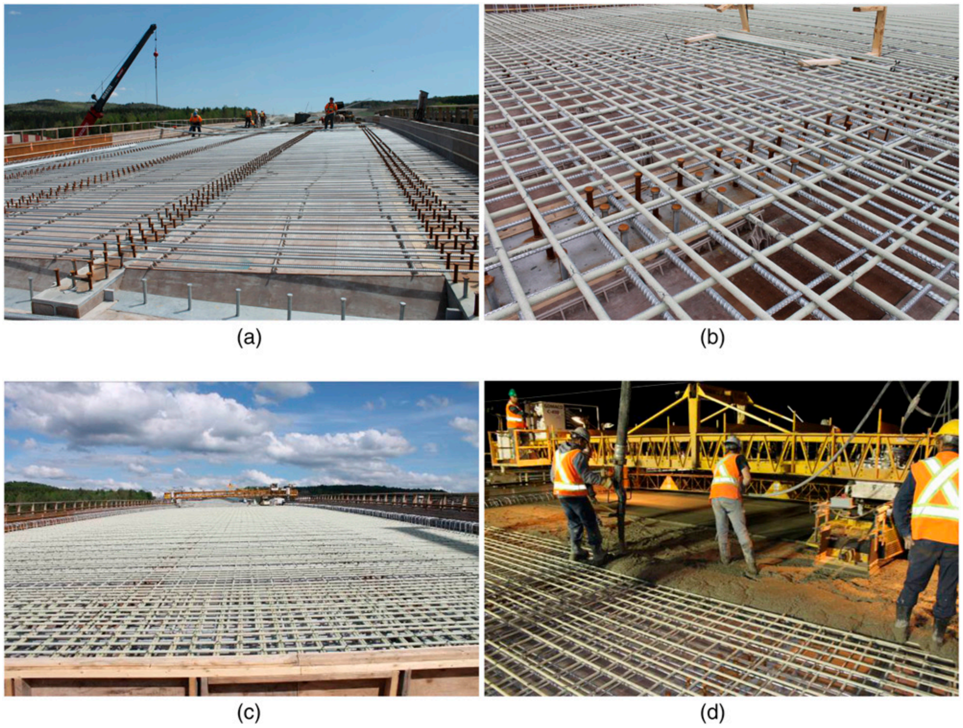

Fig. 3. Bridge construction: (a) bottom reinforcing steel; (b) bottom and top reinforcement; (c) completed reinforcement of the bridge deck; (d) concrete casting (images by the authors)

Table 1. Properties of the Glass Fiber–Reinforced Polymer and Steel Reinforcing Bars

Reinforcing bar type	Grade[a]	Bar size[a]	Area[a] (mm^2)	Elastic tensile modulus E_f (GPa)	Ultimate tensile strength (MPa)	Characteristic tensile strength[b] (MPa)	Ultimate tensile elongation (%)
Glass fiber–reinforced polymer	II	Number 20	284	54.3 ± 0.8	$1{,}393 \pm 8$	1,369	2.56
Steel	—	15M	200	200	$f_y = 400$[c]	—	—
	—	20M	300	200	$f_y = 400$[c]	—	—

[a]According to CSA (2010).
[b]Characteristic tensile strength = average value – 3 × standard deviation (CSA 2012).
[c]The quantity f_y is the yield strength of steel bars.

minimum area specified by the CSA (2006). The bottom longitudinal reinforcement was set to the minimum reinforcement level, which is 15M steel bars at 300 mm. On the other hand, the area of GFRP bars in the top longitudinal and transverse directions was equal to $0.0035 \times d_s \times 1{,}000$, which yields No. 15 GFRP bars at 300 mm (minimum reinforcement). Furthermore, if the deck slabs were totally reinforced with GFRP bars, the empirical design method would have yielded No. 20 GFRP bars at 175 mm ($500d_s/E_{\mathrm{FRP}}$) in the bottom transverse directions and No. 15 GFRP bars at 300 mm in all other directions.

Comparing the designs with the empirical method to that of the flexural method reveals that the empirical method saves up to 25% of the transverse reinforcement (in those bridges). This could be justified, because when the bridge deck slab meets the requirements of the empirical method, the arch action has a significant effect, which contributes to reducing the reinforcement amount.

Instrumentation

The P-15502S bridge (Fig. 1) was instrumented with Fabry-Perot FOSs at critical locations to record the reinforcement strains. Instrumentation was distributed along the midspan section of the bridge, as shown in Fig. 4. The FOSs were glued to the transverse GFRP reinforcing bars in the top mat and the transverse steel bars in the bottom mat. The FOSs were glued to the GFRP bars (T1–T5) at the locations of support girders (maximum negative moment) and to the steel bars (B1–B4) at the centerlines between the support girders (maximum positive moment) (Fig. 4). The GFRP and steel bars were instrumented at the structural laboratory of the University of Sherbrooke. Thereafter, the bars were shipped to the construction site, where they were installed in the designated locations. Fig. 5 shows both the instrumentation of the reinforcing bars and the installation of the instrumented bars in the field. The objective of using FOSs was to allow for the long-term monitoring and future field testing of the bridge. The Fabry-Perot FOSs used were manufactured by Roctest (Saint-Lambert, Quebec, Canada).

During static tests of the P-15502S bridge, the deflection of the steel girders was measured (D1–D5) with a theodolite and a system of rulers installed at the bridge midspan (Fig. 3). The deflection was also measured with two general-purpose digital-contact sensors with a 50-mm range (GT2-H50) located at D2 and D4 (Beams 2 and 4; Fig. 2). Fig. 6 shows the ruler system and the two GT2-H50 sensors during bridge testing. The GT2-H50 sensors were manufactured by Osmos Canada (Montréal, Quebec, Canada).

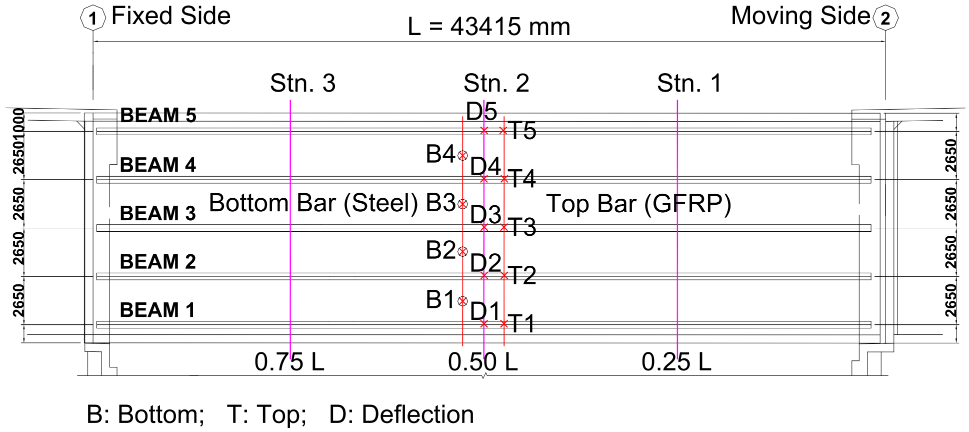

Fig. 4. Instrumentation for strain and deflection measurements

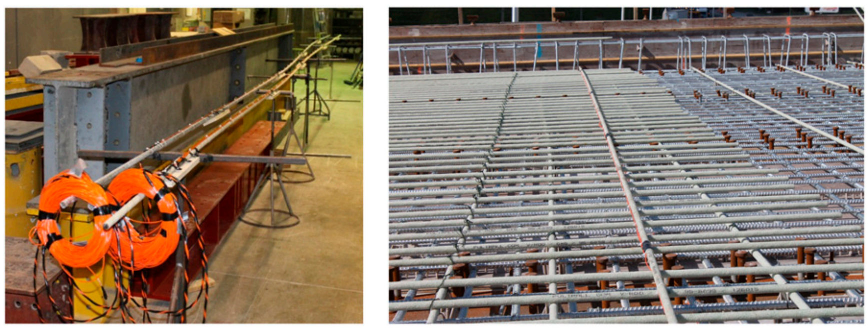

Fig. 5. Instrumentation and installation of the reinforcing bars (images by the authors)

Fig. 6. Deflection measurements using rulers and GT-H50 sensors (images by the authors)

Early-Age Strain Evolution in the Reinforcing Bars

After concrete casting, the early-age strains in the instrumented reinforcement of the P-15502S bridge and their evolution with time were monitored. The FOS readings were recorded from May 31, 2012 (initial reading before concrete casting) to July 12, 2012 (two weeks after formwork removal). Fig. 7 shows the strain evolution in the transverse steel and GFRP bars at the midspan of the P-15502S bridge.

As illustrated in Fig. 7, during the first week, the concrete showed shrinkage cracking, which was captured with the FOSs attached to the reinforcing bars (steel and GFRP). Consequently, the reinforcing bars showed compressive strains. The removal of the formwork of the P-15502S bridge was started on June 13 and completed by June 29, 2012. The effect of removing the formwork (application of the dead load of the slabs) was observable. When the removal started, the bottom transverse steel bars showed tensile strain, whereas the top transverse GFRP bars showed very small tensile or compressive strain. This confirms the arching action in the restrained hybrid-reinforced-concrete bridge-deck slabs.

After the bridge's side barriers were cast, some tools and materials were placed on the bridge in the area between Beams 3 and 5 (Fig. 4), which affects the induced strains. The maximum tensile strain in the bottom transverse steel bars was about 165 microstrains (Gauge B4), whereas the maximum tensile strain in the top transverse GFRP bars was 21 microstrains (Gauge T3).

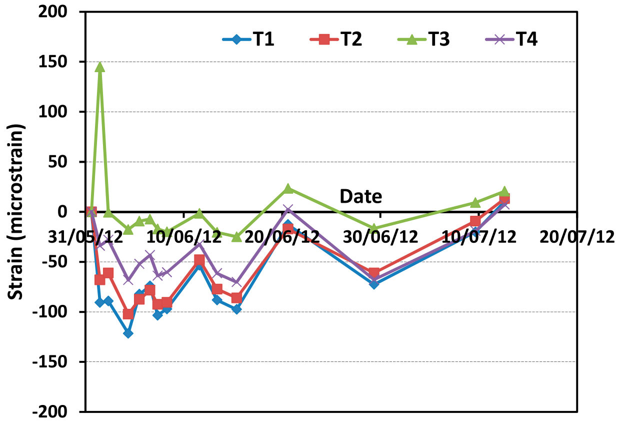

(a) Top transverse GFRP bars

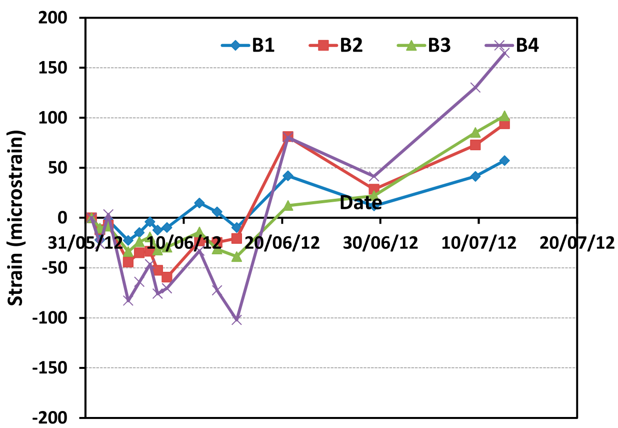

(b) Bottom transverse steel bars

Fig. 7. Early-age strain evolution in the reinforcing bars under dead load: (a) top transverse GFRP bars; (b) bottom transverse steel bars

Live-Load Testing of the P-15502S Bridge

The P-15502S bridge was tested on October 30, 2012, for service performance, as specified by the CSA (2006) using three three-axle calibrated trucks. Trucks 1–3 had loads of about 72 kN on the front axle and approximately 88 kN on each back axle. Fig. 8(a) illustrates the trucks. The bridge deck was tested along six loading paths using one, two, and three trucks at three different stations (truck stops) in the bridge's longitudinal direction (Stations 1–3). The stations were selected at the quarter-points and midpoint of the bridge to capture variations in the straining actions according to the truck locations on the bridge. The six loading paths, shown in Fig. 8(b), were marked on the bridge deck as were the three stations. Readings were recorded at a truck station when the midpoint of the truck's second and third axles was directly over the station. Fig. 9 shows the trucks on the bridge during testing.

Live-Load Test Results

After each loading pass, the deck slab of the P-15502S bridge was visually checked for any signs of cracking over the girders (negative-moment areas). No cracks were observed at any location in the top surface of the bridge deck at the girder locations.

Strain Measurements

Fig. 10 shows strain variation in the bottom transverse steel bars and the top transverse GFRP bars according to truck location on the bridge. The maximum strains were recorded when the trucks stopped in the middle of the bridge (Station 2). Fig. 11 presents the maximum strains resulting from the different loading paths when the trucks were in the middle of the bridge. Generally, the strains were very low in the bottom transverse steel bars and top transverse GFRP bars. The strain in the bottom transverse steel bars at its maximum location was 15 microstrains, and the strain in the top transverse GFRP bars

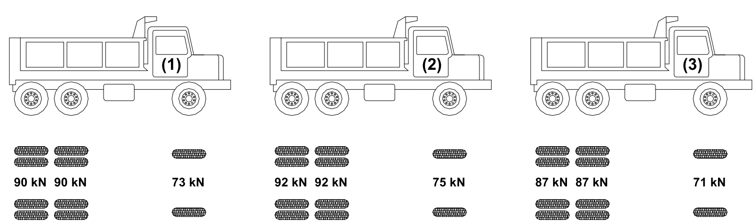

(a) Truck loads

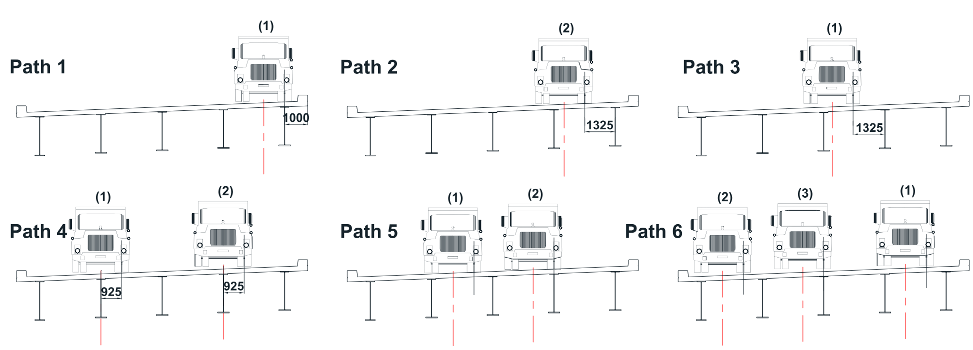

(b) Testing paths

Fig. 8. Truck loads and loading paths in cross section during testing: (a) truck loads; (b) testing paths

Fig. 9. Trucks during testing (images by the authors)

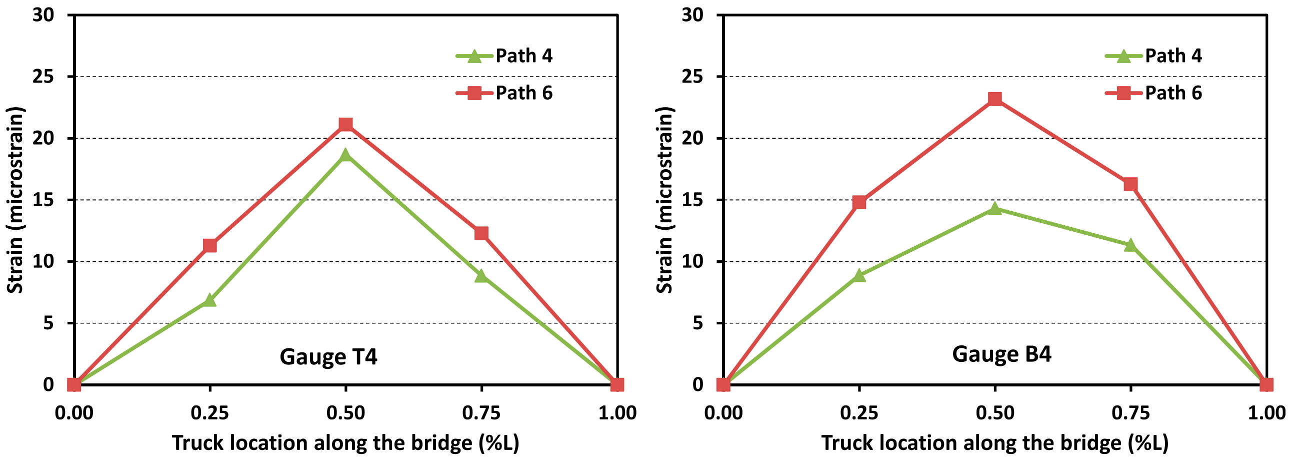

Fig. 10. Variation of strains according to truck location

reached a maximum of 25 microstrains. It should be noted that strains in steel reinforcing bars of the same order as those measured in this paper were reported for similar bridges that were constructed using FRP or steel bars in their concrete deck slabs (El-Salakawy et al. 2003b, 2005; Benmokrane et al. 2006, 2007).

The maximum measured tensile strains in the GFRP bars were less than 1% of the GFRP's ultimate strains (1,390/54,300 = 25,600 microstrains). The design service load of 110.25 kN [specified by the CSA (2006)] is approximately 2.5 times greater than the maximum wheel load of 45 kN [Fig. 8(a)] for the trucks used in the field test. If the maximum values of the strains measured in the field are linearly extrapolated (multiplied by 2.5), however, the resulting values for the tensile strains will be about 63 microstrains in the top transverse GFRP bars. These values are still less than 1% of the ultimate strains of the GFRP bars. According to the CSA (2006), the allowable stress or strain limit for GFRP bars in concrete slabs is 25% of the material's ultimate stress or strain values. Similar extrapolation of the strains in the bottom transverse steel bars yielded a strain value of about 2% of the ultimate strain capacity of the steel bars (based on a yield strain of 2,000 microstrains), which is also very low.

The very small measured strains (Fig. 11) indicate the presence of arching action in the restrained hybrid-reinforced-concrete bridge-deck slabs. Although the bridge deck was designed according to the CHBDC's flexural design method (CSA 2006), the slabs did not show real flexural response attributable to the arch-action effect. Furthermore, because the bridge deck meets CHBDC requirements (CSA 2006) for the empirical method, it was possible to design it using the empirical method. The bridge deck's design based on the empirical method yields 15M steel bars at 300 mm as bottom transverse reinforcement (minimum reinforcement), 15M steel bars at 300 mm (minimum reinforcement) as bottom longitudinal reinforcement, and No. 15 GFRP bars at 300 mm (minimum reinforcement) as top transverse and longitudinal reinforcement. This design saves a significant amount of transverse reinforcement (steel and GFRP bars) compared with the design using the flexural method.

Deflection Measurements

Fig. 12(a) shows the variation of the measured deflection of the steel girders with the truck location along the bridge, whereas Fig. 12(b) presents the deflection of the steel girders at the bridge midspan attributable to trucks located at the midspan (Station 2) for the different paths. The measured deflection indicates that the truck loading was not evenly distributed on the steel girders. The girder closest to the loading path deformed more than those further away. This was more obvious when the truck traveled over or near the edge girder. As shown in Fig. 12(b), the single truck following Path 1 [over Girder 5 on the edge; see Fig. 8(b)] produced the peak deflection in Girder 5 of 12.0 mm ($L/3{,}617$). The peak deflection with the two calibrated trucks traveling simultaneously along Paths 4 and 5 was 14.0 mm ($L/3{,}101$) in Girder 2. Furthermore, as noted with Paths 4 and 5, the deflection distribution was better when the load was applied to two lanes, as evidenced by Fig. 12(b).

Fig. 13 shows the continuous deflection measurements for Beams 2 and 3 using the G2-H50 sensors during the field test. Comparing the results presented in Figs. 12 and 13 reveals that the conventional rulers and theodolite system yielded deflection measurements very close to that provided by the G2-H50 sensors. Considering Path 6 and Station 2, the deflection of Beam 2 was 20.5 mm according to the rulers and theodolite system [Fig. 12(b)] and 19.51 mm according to the G2-H50 sensors (Fig. 13). Thus, this system may be a viable tool when such advanced techniques are not available. Advanced optical sensors, however, have the advantage of being able to capture the dynamic response when needed.

Live-Load Distribution Factors

Many techniques are available to determine transverse live-load distribution or girder distribution factors (DFs). Zokaie et al. (1991) grouped analytical techniques into three different levels of analysis from detailed modeling to simplified equations. Field testing can also provide information on live-load DFs for a given bridge type and geometry (Kim and Nowak 1997; Barr et al. 2001; Eom and Nowak 2001; Schwarz and Laman 2001). The DFs can be determined from field measurements using

$$\mathrm{DF}_i = \delta_i / \sum \delta_i \quad (1)$$

where δ_i = maximum static deflection in the ith girder.

The deflection measurements shown in Fig. 12 for the P-15502S bridge were used to determine the live-load distribution factors according to Eq. (1). From AASHTO (2012), live-load distribution factors are provided that can be compared with the measured DFs. The exterior girder (Beam 5; Fig. 1) deflected 12 mm under loading Path 1. The total deflection of all of the girders was 33 mm for a live-load DF of about 12/32 or 0.38. The AASHTO (2012) live-load distribution factors are 0.65 using the lever rule and 0.46 with special analysis. These factors are based on load and bridge geometry and exclude the 1.2 multiple presence factor (AASHTO 2012, Article 4.6.2.2.2d). The interior girder (Beam 3; Fig. 1) deflected 7 mm under loading Path 3 (Fig. 12). The total deflection of all of the girders was 28 mm for a live-load distribution factor of about 7/28 or 0.25. The AASHTO (2012) live-load distribution factor is 0.45. The live-load distribution factor depends on girder spacing, span length, and girder rigidity. Thus, it may be concluded that the DFs of AASHTO (2012) tend to be more conservative than the measured values.

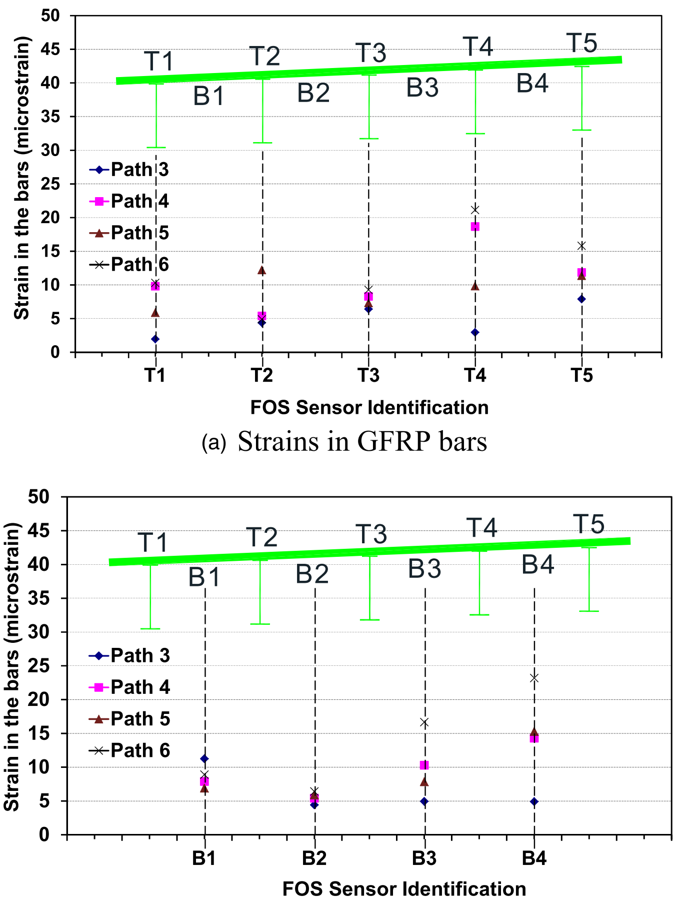

(a) Strains in GFRP bars

(b) Strains in steel bars

Fig. 11. Reinforcement strains: (a) strains in GFRP bars; (b) strains in steel bars

Conclusions

This paper presents the construction details and the live-load field testing of the hybrid-reinforced Sainte Catherine overpass located on Highway 410 (Sherbrooke, Quebec). Based on the details presented in this paper and the results of the field-loading test, the following conclusions can be drawn:

- The maximum tensile strain in the top transverse GFRP bars was less than 1% of the ultimate tensile strain of the GFRP bars. Nevertheless, it is lower than the strains expected with the flexural design method. This result suggests that the CSA (2006) flexural design method overestimates the calculated design moments.
- The very small measured strains in the GFRP reinforcing bars indicate the presence of arching action between the girders in the

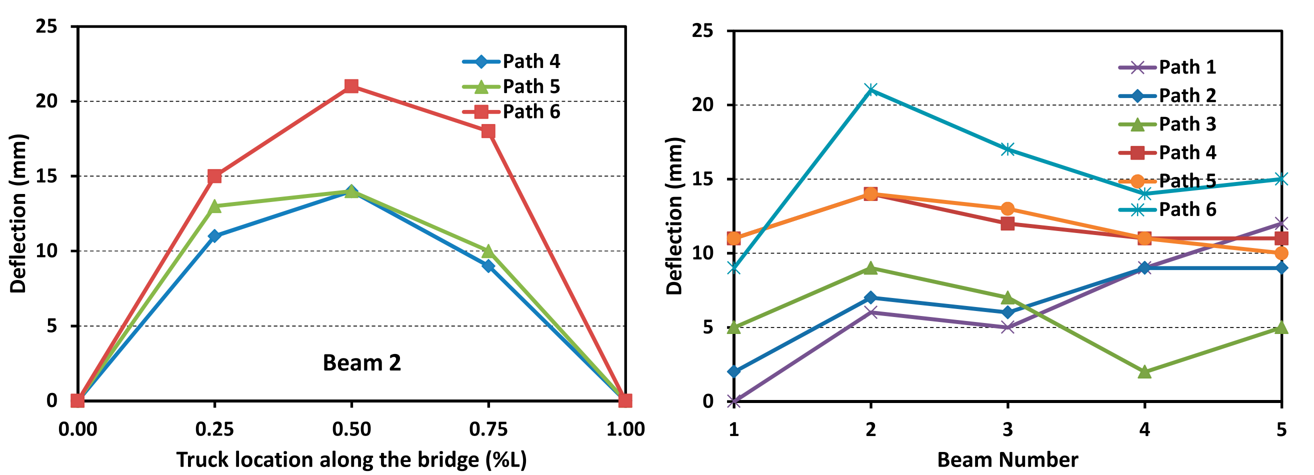

(a) Variation with the truck location

(b) Deflection of all girders

Fig. 12. Maximum measured deflection of steel girders (trucks at midspan; Station 2): (a) variation with the truck location; (b) deflection of all girders

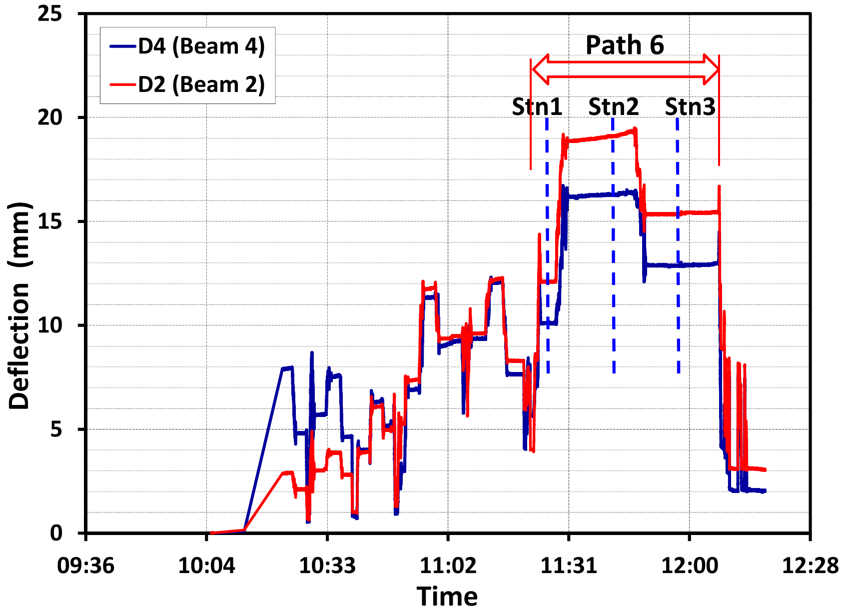

Fig. 13. Measured deflection of steel girders using G2-H50 sensors

restrained hybrid-reinforced-concrete bridge decks. In the unlikely occurrence of field failure, the mode would be punching shear.

- When hybrid-reinforced-concrete bridge decks meet the CHBDC requirements (CSA 2006) concerning the empirical design method, they could be designed accordingly, which could save significant amounts of transverse reinforcement.
- The conventional rulers and theodolite system may be a viable method to measure the deflection of bridge girders during field testing when advanced systems are not available. This would not apply, however, if the dynamic response were of interest.
- The DFs of AASHTO (2012) tend to be more conservative than the measured values.
- The tests conducted in this paper confirmed that the behavior of hybrid-reinforced-concrete bridge decks is similar to that totally reinforced with FRP or steel bars. This hybrid concept may be a viable solution for concrete bridge decks with extended service life.
- The continuous monitoring of the bridge deck will enable understanding of the long-term structural behavior and performance in real environmental and service conditions. The results of such applications along with the compelling evidence presented on the durability of GFRP reinforcement from bridges in different environments (Mufti et al. 2005, 2007; 2011) encourage wider acceptance of this technology. They will also lead to cost-effective design of concrete structures/bridges with extended service life.

Acknowledgments

This research received financial support from the Natural Science and Engineering Research Council of Canada (NSERC), the Fonds québécois de la recherche sur la nature et les technologies (FQRNT), and the Ministry of Transportation of Quebec (MTQ). The authors are also grateful to CIMA+ (Sherbrooke, Quebec, Canada), the S. M. Group International. (Sherbrooke, Quebec, Canada), Sintra (Sherbrooke, Quebec, Canada), and the technical staff of the structural laboratory at the University of Sherbrooke, especially Martin Bernard and Simon Kelly, for their assistance in instrumenting and testing the bridge.

References

AASHTO. (2012). *LRFD bridge design specifications*, 6th Ed., Washington, DC.

Ahmed, E., and Benmokrane, B. (2012). "Hybrid reinforced concrete bridge deck slab of 410 Overpass Bridge in Quebec: Construction and testing." *Proc., 3rd Int. Structural Specialty Conf.*, Canadian Society for Civil Engineering, Montreal.

Ahmed, E. A., and Benmokrane, B. (2011). "Static testing of full-scale concrete bridge barriers reinforced with GFRP bars." *Proc., 10th Int. Symp. on Fiber-Reinforced Polymer Reinforcement for Concrete Structures (FRPRCS-10)*, R. Sen et al., eds., American Concrete Institute, Farmington Hills, MI, 5.1–5.20.

Ahmed, E. A., Dulude, C., and Benmokrane, B. (2013). "GFRP-reinforced concrete bridge barriers: Static tests and pendulum impacts." *Can. J. Civ. Eng.*, 40(11), 1050–1059.

Barr, P. J., Eberhard, M. O., and Stanton, J. F. (2001). "Live-load distribution factors in prestressed concrete girder bridges." *J. Bridge Eng.*, 10.1061/(ASCE)1084-0702(2001)6:5(298), 298–306.

Benmokrane, B., El-Salakawy, E., Desgagné, G., and Lackey, T. (2004). "FRP bars for bridges." *Concr. Int.*, 26(8), 84–90.

Benmokrane, B., El-Salakawy, E., El-Gamal, S., and Goulet, S. (2007). "Construction and testing of Canada's first concrete bridge deck totally reinforced with glass FRP bars: Val-Alain bridge on Highway 20 East." *J. Bridge Eng.*, 10.1061/(ASCE)1084-0702(2007)12:5(632), 632–645.

Benmokrane, B., El-Salakawy, E. F., El-Ragaby, A., and Lackey, T. (2006). "Designing and testing of concrete bridge decks reinforced with glass FRP bars." *J. Bridge Eng.*, 10.1061/(ASCE)1084-0702(2006)11:2(217), 217–229.

Canadian Standards Association (CSA). (2006). "Canadian highway bridge design code." *CAN/CSA S6–06*, Rexdale, ON, Canada.

Canadian Standards Association (CSA). (2010). "Specification for fibre-reinforced polymers." *CAN/CSA S807–10*, Rexdale, ON, Canada.

Canadian Standards Association (CSA). (2012). "Design and construction of building structures with fibre reinforced polymers." *CAN/CSA S806–12*, Rexdale, ON, Canada.

Eamon, D. C., Jensen, E. A., Grace, N. F., and Shi, X. (2012). "Life-cycle cost analysis of alternative reinforcement materials for bridge superstructures considering cost and maintenance uncertainties." *J. Mater. Civ. Eng.*, 10.1061/(ASCE)MT.1943-5533.0000398, 373–380.

El-Gamal, S., El-Salakawy, E., and Benmokrane, B. (2005). "Behavior of concrete bridge deck slabs reinforced with fiber-reinforced polymer bars under concentrated loads." *ACI Struct. J.*, 102(5), 727–735.

El-Gamal, S., El-Salakawy, E., and Benmokrane, B. (2007). "Influence of reinforcement on the behavior of concrete bridge deck slabs reinforced with FRP bars." *J. Compos. Constr.*, 10.1061/(ASCE)1090-0268(2007)11:5(449), 449–458.

El-Ragaby, A., El-Salakawy, E., and Benmokrane, B. (2007a). "Fatigue analysis of concrete bridge deck slabs reinforced with E-glass/vinyl ester FRP reinforcing bars." *Composites Part B*, 38(5–6), 703–711.

El-Ragaby, A., El-Salakawy, E., and Benmokrane, B. (2007b). "Fatigue life evaluation of concrete bridge deck slabs reinforced with glass FRP composite bars." *J. Compos. Constr.*, 10.1061/(ASCE)1090-0268(2007)11:3(258), 258–268.

El-Salakawy, E., Benmokrane, B., Masmoudi, R., Brière, F., and Breaumier, E. (2003a). "Concrete bridge barriers reinforced with glass fiber-reinforced polymer composite bars." *ACI Struct. J.*, 100(6), 815–824.

El-Salakawy, E., Masmoudi, R., Benmokrane, B., Brière, F., and Desgagné, G. (2004). "Pendulum impacts into concrete bridge barriers reinforced with glass fibre reinforced polymer composite bars." *Can. J. Civ. Eng.*, 31(4), 539–552.

El-Salakawy, E. F., and Benmokrane, B. (2003). "Design and testing of a highway concrete bridge deck reinforced with glass and carbon FRP bars." *Field applications of FRP reinforcement: Case studies*, American Concrete Institute, Detroit, 37–54.

El-Salakawy, E. F., Benmokrane, B., and Desgagné, G. (2003b). "FRP composite bars for the concrete deck slab of Wotton bridge." *Can. J. Civ. Eng.*, 30(5), 861–870.

El-Salakawy, E. F., El-Ragaby, A., and Nadeau, D. (2005). "Field investigation on the first bridge deck slab reinforced with glass FRP bars constructed in Canada." *J. Compos. Constr.*, 10.1061/(ASCE)1090-0268(2005)9:6(470), 470–479.

Eom, J., and Nowak, A. S. (2001). "Live load distribution for steel girder bridges." *J. Bridge Eng.*, 10.1061/(ASCE)1084-0702(2001)6:6(489), 489–497.

Kim, S., and Nowak, A. S. (1997). "Load distribution and impact factors for I-girder bridges." *J. Bridge Eng.*, 10.1061/(ASCE)1084-0702(1997)2:3(97), 97–104.

Mufti, A., et al. (2005). "Durability of GFRP reinforced concrete in field structures." *Proc., 7th Int. Symp. on Fiber-Reinforced Polymer (FRP) Reinforcement for Concrete Structures (FRPRCS)*, American Concrete Institute, Farmington Hills, MI, 1361–1378.

Mufti, A., Banthia, N., Benmokrane, B., Boulfiza, M., and Newhook, J. (2007). "Durability of GFRP composite rods." *Concr. Int.*, 29(2), 37–42.

Mufti, A. A., and Neale, K. W. (2007). "State-of-the-art of FRP and SHM applications in bridge structures in Canada." *Proc., Composites & Polycon 2007*, American Composites Manufacturers Association (ACMA), Arlington, VA.

Mufti, A. A., Newhook, J., Benmokrane, B., Tadros, G., and Vogel, H. M. (2011). "Durability of GFRP rods in field demonstration projects across Canada." *Proc., 4th Int. Conf. on Durability & Sustainability of Fibre Reinforced Polymer (FRP) Composites for Construction and Rehabilitation of Structures (CDCC2011)*, B. Benmokrane, E. El-Salakawy, and E. Ahmed, eds., Quebec City, 27–35.

Phillips, K. A., Harlan, M., Roberts-Wollmann, C. L., and Cousins, T. E. (2005). "Performance of a bridge deck with glass fiber reinforced polymer bars as the top mat of reinforcement." *Technical Rep. No. VTRC 05-CR24*, Federal Highway Administration, Washington, DC.

Schwarz, M., and Laman, L. A. (2001). "Response of prestressed concrete I-girder bridges to live load." *J. Bridge Eng.*, 10.1061/(ASCE)1084-0702(2001)6:1(1), 1–8.

Zokaie, T., Osterkamp, T. A., and Imbsen, R. A. (1991). "Distribution of wheel loads on highway bridges." *Final Rep. NCHRP 12-26/1*, National Cooperative Highway Research Program, Washington, DC.